Near-circularly polarized isolated attosecond pulse generation from coherent superposition state by a circularly polarized laser field

Hua Yuan[1] · Feng Wang[2] · Yinfu Zhang[1] · Renzhi Shao[1] · Hua Long[1]

Abstract

We theoretically investigate high-order harmonic generation (HHG) from a coherent super-position state of hydrogen atom in a circularly polarized (CP) laser field. The results show that, driven by the CP field, HHG from the coherent superposition state is enhanced by 4 to 5 orders of magnitude compared to that from the ground state. The enhanced intensity is comparable to that of the ground state in a linearly polarized laser field. Based on the classical and quantum analyses, we demonstrate that HHG in the CP laser field mainly arises from the recombination of electrons ionized at non-zero initial positions. The enhancement of HHG from the coherent superposition state is due to the higher ionization rate and also the larger probability density of electrons located far from the nucleus of the involved excited state. The obtained harmonic spectra support the generation of intense isolated attosecond pulses (IAPs) with the ellipticity as high as 0.93. Moreover, we show that the generation of IAPs with large ellipticity is robust against the variation of the carrier envelope phase (CEP) of the laser field. Our results provide a new route toward generating near-CP IAPs, which will be beneficial for ultrafast detection of chiral-sensitive light-matter interactions.

1 Introduction

High-order harmonic generation (HHG) in atoms or molecules driven by femtosecond lasers is an extremely nonlinear optical process that up-converts the intense infrared laser field into the extreme ultraviolet (EUV) and soft x-ray radiation (Popmintchev et al. 2012; Teichmann et al. 2016; Li et al. 2018). The emitted harmonics nowadays have been the

✉ Hua Long
    longhua@hust.edu.cn

1   Wuhan National Laboratory for Optoelectronics and School of Physics, Huazhong University of Science and Technology, Wuhan 430074, China

2   Hubei Key Laboratory of Optical Information and Pattern Recognition, Wuhan Institute of Technology, Wuhan 430205, China

main source to generate isolated attosecond pulses (IAPs) (Krausz and Ivanov 2009; Li et al. 2017a; Gaumnitz et al. 2017). IAPs offer unprecedented spatial and temporal resolutions in observing and controlling the ultrafast electronic dynamics inside atoms (Zhou et al. 2012; Liu et al. 2019a, b; Ma et al. 2019; Goulielmakis et al. 2010; Wang et al. 2019; Tan et al. 2018, 2019; Luo et al. 2019; Li et al. 2019a), molecules (Yuan et al. 2018; He et al. 2019; Itatani et al. 2004; Wang et al. 2018; He et al. 2018a; Qin et al. 2019; Baker et al. 2006; Lan et al. 2017; He et al. 2018b, c), solids (Ghimire et al. 2011; Li et al. 2019c; Vampa et al. 2015; Liu et al. 2018; Schultze et al. 2014; Gui et al. 2018; Li et al. 2019b), and nanostructures (Kim et al. 2008; Chen et al. 2018; krüger et al. 2018). Many methods have been proposed to generate IAPs, such as by using a few-cycle laser pulse, the polarization gating technique, the two-color or multi-color fields, the chirped laser pulse and the spatially inhomogeneous field (Kienberger et al. 2004; Sansone et al. 2006; Pfeifer et al. 2006; Feng and Chu 2011; Feng 2015; Feng et al. 2018; Ciappina et al. 2017). However, these previous studies are mainly focused on the generation of linearly polarized (LP) attosecond pulses. Beyond that, the attosecond pulse can also carry the spin angular momentum, which will provide an additional degree of freedom and offer many different applications in probing ultrafast electron dynamics. For instance, circularly (or largely elliptically) polarized attosecond pulses have been found of important uses ranging from chiral recognition and magnetic circular dichroism to time-resolved magnetization dynamics and spin currents (Böwering et al. 2001; Ferré et al. 2014; López-Flores et al. 2012; Barth and Manz 2007). For these important applications, the generation of (near-) circularly polarized (CP) attosecond pulses has been a topic of growing interest in the past few years.

To generate a CP attosecond pulse, one may consider directly using a CP driving field to interact with atoms or molecules. However, previous studies based on the analysis of the symmetry property indicate that in a perfect CP field, i.e., a monochromatic CP field, HHG from a spherical symmetric system is forbidden (Alon et al. 1998). To produce CP IAPs, some other approaches have been recently proposed (Xie et al. 2008; Yuan and Bandrauk 2013; Mauger et al. 2014; Milošević 2015; Kfir et al. 2015; Medišauskas et al. 2015; Fan et al. 2015; Dorney et al. 2017; Ellis et al. 2018; Hernández-García et al. 2016; Hickstein et al. 2015; Huang et al. 2018; Li et al. 2017b). It has been demonstrated that pure CP harmonics can be generated by using a CP fundamental driving pulse in combination with its counterrotating second harmonic (Milošević 2015; Kfir et al. 2015; Medišauskas et al. 2015; Fan et al. 2015; Dorney et al. 2017). However, in this regard, the two adjacent harmonics exhibit opposite helicities, which will reduce the ellipticity of the synthesized IAPs (Medišauskas et al. 2015). Alternatively, by crossing two CP counterrotating pulses in a noncollinear geometry, pure CP harmonics with opposite helicities can be effectively separated in space, and then IAPs with pure circular polarization can be produced in the few-cycle regime (Hernández-García et al. 2016; Hickstein et al. 2015; Huang et al. 2018). However, in the noncollinear geometry, the small interaction volume at the cross point is not beneficial for the generation of IAPs with high intensity (Hernández-García et al. 2016). Therefore, other methods to generate (near-) CP IAPs are still desired.

Recently, HHG from the coherent superposition of the ground state and an excited state of an atom (an excited atom) has attracted much attention (Hu and Collins 2004; Zhai et al. 2011; Wang et al. 2014; Zhai et al. 2010; Chen et al. 2012; Bleda et al. 2013). Compared to the ground state of the atom, the excited states have much smaller binding energy, thus HHG from excited atoms possesses much higher intensity (Hu and Collins 2004; Zhai et al. 2011). Moreover, electrons in the excited states are far from the nucleus with a large electron orbital radius. After ionization, the electrons can be accelerated directly toward the parent ion under the drive of the laser field. Such a peculiar dynamics has modulated the

HHG process and leads to some unusual phenomena, for instance, the cutoff extension in a few-cycle laser field (Zhai et al. 2011; Wang et al. 2014).

In this paper, we investigate HHG from a coherent superposition state of hydrogen atom in a CP driving field. The harmonic yield is demonstrated to be about 4 to 5 orders of magnitude higher than that from the atom in ground state (we call it ground-state atom below) in the CP field, becoming comparable to that from the ground-state atom in a LP laser field. By performing the classical and quantum simulations, we find that HHG in the CP laser field mainly arises from the recombination of electrons ionized at non-zero initial positions. The HHG enhancement is due to the higher ionization rate and also the larger probability density of electrons located far from the nucleus of the excited state. The generated harmonics can be used to produce IAPs with the ellipticity up to 0.93. Furthermore, we also discuss the influence of the carrier envelope phase (CEP) on the IAP generation. It is shown that IAPs with large ellipticity can still be generated as the CEP varies.

2 Theoretical model

In our simulations, we investigate HHG from a coherent superposition state of hydrogen atom in a CP laser field by solving the time-dependent Schrödinger equation in three spatial dimension (3D-TDSE), which reads (atomic units are used throughout unless otherwise stated),

$$i\frac{\partial \psi(\mathbf{r}, t)}{\partial t} = H(\mathbf{r}, t)\psi(\mathbf{r}, t). \tag{1}$$

The Hamilton $H(\mathbf{r}, t)$ is given by

$$H(\mathbf{r}, t) = -\frac{1}{2}\nabla^2 + V_{atom}(\mathbf{r}) + V_{laser}(t). \tag{2}$$

here $\mathbf{r} \equiv (x, y, z)$ denotes the coordinate of the electron. $V_{atom}(\mathbf{r}) = -\frac{1}{|\mathbf{r}|}$ is the coulomb potential of hydrogen atom. $V_{laser}(t) = -\mathbf{E}(t)\mathbf{r}$ is the potential due to the laser-electron interaction. The electric vector of the CP field $\mathbf{E}(t)$ is in the xy plane, which can be written as

$$\mathbf{E}(t) = E_0 f(t)[\sin(\omega_0 t + \phi_0)\mathbf{e_x} + \cos(\omega_0 t + \phi_0)\mathbf{e_y}], \tag{3}$$

where E_0 and ϕ_0 are the amplitude and CEP of the CP laser pulse, respectively. ω_0 is frequency of the laser pulse, which is given by $\omega_0 = \frac{2\pi}{T_0}$ with T_0 the optical cycle of the driving laser pulse. $f(t) = \sin^2(\frac{\pi t}{T})$ is the laser envelope. $T = 10T_0$ is the duration of the laser pulse.

In our simulations, the initial state is given by a superposition of the ground state $|1s\rangle$ and an excited state $|4p\rangle$, i.e.,

$$\psi(\mathbf{r}, t = 0) = \frac{1}{\sqrt{2}}(|1s\rangle e^{i\delta} + |4p\rangle). \tag{4}$$

here δ is the relative phase between the two states (Chen et al. 2012). We find the calculated results are insensitive to the variation of δ. For simplicity, δ has been set to be zero throughout this paper. The initial wave functions of the 1s and 4p states are calculated by means of the imaginary time propagation method. In experiments, such a superposition state can be obtained by exciting the ground state using a long laser pulse (Zhai et al. 2010),

where the peak frequency of the laser pulse is chosen to be the energy spacing between the excited and ground states, and the intensity of the laser pulse is adjusted according to the amplitude of the excited state. Besides, using multi-photon resonant excitation or electromagnetically induced transparency (Avetissian and Mkrtchian 2002; Avetissian et al. 2006; Djotyan et al. 2004), the superposition state can also be obtained. We use the split-operator method to solve Eq. (1) (Feit et al. 1982; Zhang et al. 2019). The integration grids are confined in the extents of $|x| \leq 150$ a.u., $|y| \leq 150$ a.u. and $|z| \leq 100$ a.u. with the spatial spacing of 0.4 a.u. The time step is 0.2 a.u. In order to avoid the reflections from the spatial boundaries, at each time step the electron wave function is multiplied by a mask function of the form $\cos^{\frac{1}{8}}$. Once the electron wave function $\psi(\mathbf{r}, t)$ is obtained, the time-dependent dipole acceleration along the x and y directions can be calculated with the Ehrenfest's theorem (Burnett et al. 1992)

$$
\begin{aligned}
a_x(t) &= -\langle \psi(\mathbf{r}, t) | [H(\mathbf{r}, t), [H(\mathbf{r}, t), x]] | \psi(\mathbf{r}, t) \rangle, \\
a_y(t) &= -\langle \psi(\mathbf{r}, t) | \big[H(\mathbf{r}, t), \big[H(\mathbf{r}, t), y\big]\big] | \psi(\mathbf{r}, t) \rangle.
\end{aligned}
\tag{5}
$$

The harmonic spectrum is given by the Fourier transform of the time-dependent dipole acceleration, i.e.,

$$
\begin{aligned}
\left| s_x(\omega_n) \right|^2 &= \left| \frac{1}{T} \int_0^T a_x(t) e^{-i\omega_n t} dt \right|^2, \\
\left| s_y(\omega_n) \right|^2 &= \left| \frac{1}{T} \int_0^T a_y(t) e^{-i\omega_n t} dt \right|^2,
\end{aligned}
\tag{6}
$$

with $\omega_n = \frac{2n\pi}{T}$, n=1, 2, ..., N_{max} (N_{max} is the time point). The attosecond pulse is obtained by superposing several orders of harmonics in the plateau,

$$
\begin{aligned}
I_x(t) &= \left| \sum_q s_x e^{iq\omega_0 t} \right|^2, \\
I_y(t) &= \left| \sum_q s_y e^{iq\omega_0 t} \right|^2.
\end{aligned}
\tag{7}
$$

here q corresponds to the harmonic order.

3 Results and discussion

In our simulations, a 1300-nm CP laser field with the intensity of 2.0×10^{14} W/cm^2 is chosen as the driving field. Figure 1a shows the electric field. Here, the CEP is set to be $\phi_0 = 0$. Figure 1b shows the x, y components of the harmonic spectrum generated from the excited hydrogen atom in this CP laser field (the red solid and green dotted lines). For comparison, the results from the ground-state atom in the CP (the red dash-dotted and green dashed lines) and LP (the yellow solid line) laser fields are also presented. Here, it should be explained that in our simulations, we use a pulsed CP field, which is
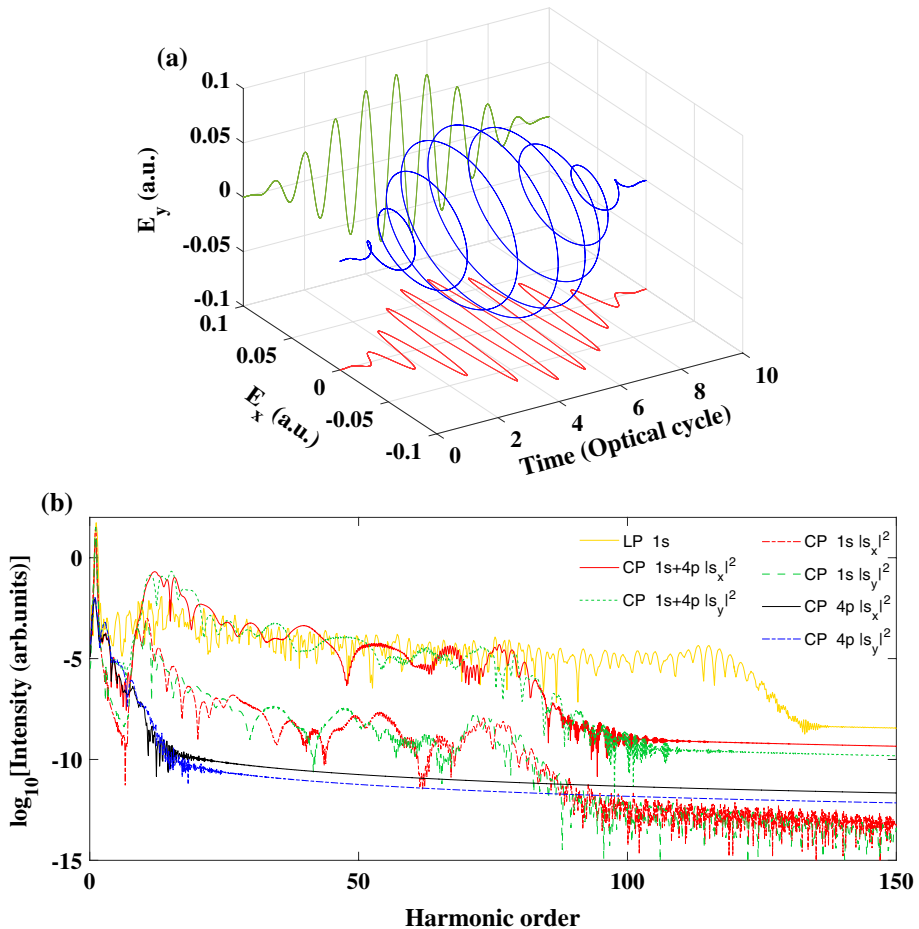
Fig. 1 (Color online) **a** The 3D plot of the CP field (blue line). The *x*, *y* components of the electric field are shown as the red and green lines, respectively. **b** The x, y components of the generated harmonic spectrum from the excited hydrogen atom (the red solid and green dotted lines) in the CP laser field. For comparison, the results from the ground-state atom (the red dash-dotted and green dashed lines), the pure excited state (the black solid and blue dash-dotted lines) in the CP laser field and the ground-state atom in the LP laser field (the yellow solid line) are also presented. In our simulations, the electric amplitude and other parameters of the LP laser field are the same as that of the CP laser field

not a perfect (monochromatic) CP field. The time-dependent laser envelope will break the dynamical symmetry of the laser field (Barreau et al. 2018; Jiménez-Galán et al. 2017). Therefore, even though we use a spherical symmetric 1s state in the simulation, we can still find harmonic emission but with low efficiency in this pulsed CP field [as shown in Fig. 1b]. Note that similar results have also been observed in HHG from atoms in a bichromatic CP field, of which the three-fold dynamical symmetry can also be broken by the time-dependent laser envelope, thus leading to the weak emission of 3n-th harmonics (Barreau et al. 2018; Jiménez-Galán et al. 2017). From Fig. 1b, one can see that the general features of harmonic spectra (both *x*, *y* components) from the excited atom are similar to those from the ground-state atom. But the intensity of HHG from the excited atom is about 4 to 5 orders of magnitude higher than that from the ground-state

atom in the CP field, which is comparable to that from the ground-state atom in the LP field.

HHG from the excited hydrogen atom, i.e., the coherent superposition state 1s+4p, may originate from the following four aspects: (I) recombination of electrons ionized from 1s state into the 1s state, i.e., the pure 1s contribution; (II) recombination of electrons ionized from 4p state into the 4p state, i.e., the pure 4p contribution; (III) recombination of electrons ionized from 1s state into the 4p state; (IV) recombination of electrons ionized from 4p state into the 1s state. As shown in Fig. 1b, HHG from the pure 1s state is much weaker than that from the superposition state, which therefore is not the main contribution to the harmonic emission from the excited atom. We have also calculated HHG from the pure 4p state (the black solid and blue dash-dotted lines). Under the laser conditions in our work, the 4p state is fully ionized within the first optical cycle of the driving field. HHG from the pure 4p state mainly occurs within the first laser cycle where the intensity of the laser pulse is very low. As a consequence, the ionized electrons gain very small kinetic energies in the acceleration process and only contribute to the generation of the first few order harmonics (below the 8th harmonic), which will not influence the harmonic emission in the plateau. Furthermore, due to the quick depletion of the 4p state and the smaller ionization rate of the 1s state, the recombination of electrons ionized from 1s state into the 4p state contributes little to the HHG. Note that the electron transition from 4p to 1s states may also occur during the HHG process. However, due to the fixed energy difference between the 1s and 4p states, the electron transition between these two states only contributes to the emission of a specific harmonic, i.e., the 13rd harmonic, whose photon energy just corresponds to the energy difference of these two states. From the above, we can then conclude that HHG in the plateau from the excited hydrogen atom mainly arises from the recombination of the electrons, removed from the 4p state, into the 1s state.

For a deep insight of HHG into the excited hydrogen atom in the CP laser field, we next study the classical electron trajectories with the method introduced in Ref. Zhai et al. (2011), Wang et al. (2014), Zhai et al. (2010), Chen et al. (2012), where the electron is assumed to be ionized at the beginning of the laser field from a non-zero initial position with a zero initial velocity due to the fact that electrons in the excited state are usually far from the core and weakly bound. In Fig. 2a, we present the trajectory of the electron ionized initially from the original point [see the solid line]. One can see that the electron driven by the CP field moves circularly around the parent ion (at the original point, marked by the black dot) with the radius changing with the amplitude of the laser field. During the motion, the electron passes through the y axis (i.e., $x = 0$) at $t = \frac{N}{2}T_0$ (N is a positive integer) [see the dash-dotted line in Fig. 2b which shows the x component of the electron trajectory], and passes through the x axis (i.e., $y = 0$) at $t = (\frac{N}{2} + \frac{1}{4})T_0$ [see the solid line in Fig. 2b which shows the y component of the electron trajectory]. Therefore, there is no a moment that the electron can be forced back to the parent ion. This means that the electron ionized from the original point will not contribute to the harmonic emission.

However, for the excited atom, the electrons in the excited state spread over a wide space region. The electron ionized far from the parent ion is likely to return to the parent ion at some specific moments if the electron displacement can equal to its initial excursion with respect to the original point. We have calculated the classical trajectories for electrons ionized from the y axis. The results show that for electrons ionized at a proper position on the positive-y axis, it can be driven back to the parent ion at $t = (N + \frac{1}{2})T_0$, where N is determined by the initial position of the electron. While for electrons ionized from the negative-y axis, the recollision will occur at $t = NT_0$. As an example, we have presented the results of $y = 60$ a.u. (dotted line) and $y = -63$ a.u. (dashed line) in Fig. 2a, b. In these two
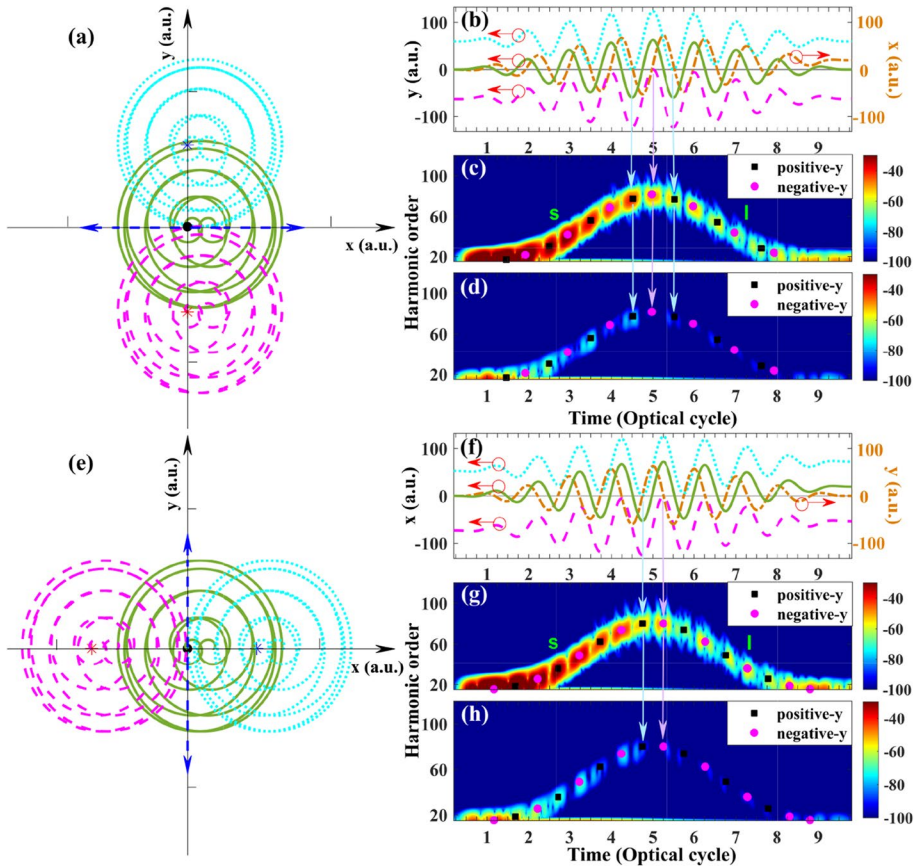
Fig. 2 (Color online) **a** Classical trajectories of the electrons ionized initially from the y axis in the CP laser field. The solid, dotted, and dashed lines correspond to initial positions at the original point, $y = 60$ a.u. and $y = -63$ a.u., respectively. The blue double-headed arrow marks the recolliding directions of the electrons. **b** The x and y components of the classical trajectories in **a**. Note that for electrons ionized from the y axis, the x components of these classical trajectories are the same (dash-dotted line). **c** The time–frequency analysis of the x component of the harmonic spectrum from the excited hydrogen atom. For comparison, the classical electron kinetic energies are also presented as a function of the recombination time. Squares and dots correspond to the results from the positive- and negative-y axes, respectively. 's' and 'l' mark the short and long quantum paths, respectively. **d** Same to **c**, but for the ground-state atom. **e–h** Same to **a–d**, but for the electrons ionized initially from the x axis. Squares and dots in **g** and **h** correspond to the classical electron kinetic energies from the positive- and negative-x axes, respectively

cases, the x components of the electron trajectories are the same to that from the original point [the dash-dotted line in Fig. 2b]. The electron ionized at $y = 60$ a.u. recollides with the parent ion at $4.5\,T_0$ and $5.5\,T_0$, i.e., where the electron displacements along both the x and y directions are 0 [see the dotted and dash-dotted lines in Fig. 2b]. While for $y = -63$ a.u., the electron returns at $5\,T_0$ [see the dashed and dash-dotted lines in Fig. 2b]. All these returning electrons will come back to the parent ion with a horizontal velocity (along the x axis, marked by the double-headed arrow), which will therefore contribute to the harmonic emission along the x direction. To check this point, we have performed the time-frequency analysis of the x component of the harmonic spectrum from the excited atom in Fig. 2c.

For comparison, the classical electron kinetic energies as a function of the recombination time are also presented (squares and dots). It's obvious that the classical results agree well with the quantum analysis. In particular, the harmonics with specific photon energies will emit every half optical cycle. For two adjacent half optical cycles, the harmonic emission just corresponds to the recombination of electrons ionized from the positive- and negative-y axes, respectively.

Similar results have also been found for electrons initially located on the x axis. The electrons on the positive- (or negative-) x axis are demonstrated to return at $t = (N + \frac{3}{4})T_0$ (or $t = (N + \frac{1}{4})T_0$). This has been verified by the results of $x = 53$ a.u. (the dotted line) and $x = -73$ a.u. (the dashed line) shown in Fig. 2e, f, where the electrons are shown to return at $t = 4.75T_0$ and $t = 5.25T_0$, respectively. In these cases, the electrons return to the parent ion with a vertical velocity (along the y axis, marked by the double-headed arrow), thus leading to the harmonic emission along the y direction. As shown in Fig. 2g, the classical results show good agreement with the time frequency analysis of the y component of HHG from the excited atom.

Based on the above analyses, we can conclude that HHG from the excited atom is mainly contributed by the electrons ionized far from the nucleus. More importantly, we note that our above classical analyses are also applicable for HHG from the ground-state atom. The classical simulations also agree well with the quantum analysis of HHG from the ground-state atom [see Fig. 2d, h]. Such an agreement indicates that HHG from the ground-state atom in the CP field can also be attributed to the recombination of the electrons ionized at non-zero initial positions, which is similar to that from the excited atom. As discussed above, the electrons driven by the CP field move circularly around the parent ion. The electric field force provides the centripetal force of the circular motion. The period of the circular motion is equal to that of the revolution of the electric field vector, i.e., one laser cycle. Then the equation of the electron motion can be described by $E = \omega_0 v$, where ω_0 is the laser frequency (i.e., the angular frequency of the circular motion), v is the velocity of the electron. The kinetic energy of the electron is given by $E_k = \frac{1}{2}v^2 = \frac{E^2}{2\omega_0^2}$. The maximum kinetic energy that the electron gained in the laser field is $E_{kmax} = \frac{E_0^2}{2\omega_0^2} = 2U_p$, where $U_p = \frac{E_0^2}{4\omega_0^2}$ is the pondermotive energy. According to the conversion of energy, the maximum energy of the emitted photon, i.e., the harmonic cutoff in the CP laser field, is $2U_p + I_p$, where I_p is the ionization potential of the ground state of the hydrogen atom. Driven by the CP laser field, the classical electron trajectories are the same for the excited and ground-state atoms, the harmonic cutoffs in these two cases are the same, which is about the 80th harmonic, agreeing well with the results in Fig. 1b. It should be stressed that in our simulations, no matter which excited state is used, the classical electron trajectories and the maximum kinetic energies that the electrons gained in the laser field are the same. Therefore, the harmonic cutoffs for all excited states are the same.

The enhancement of HHG from the excited hydrogen atom in the CP laser field mainly originates from two factors. On the one hand, the excited state possesses much higher ionization rate than the ground state due to the smaller ionization potential. As a consequence, HHG from the excited atom is obviously enhanced as seen in Fig. 1b. On the other hand, the excited state has a much larger probability density for electrons located far from the nucleus, which is also responsible for the enhancement of HHG from the excited atom. To verify this point, in Fig. 3, we show the radial density distribution of the ground (1s, the solid line) and excited (4p, the dashed line) states. One can see that the electron probability density of the ground-state atom (1s state) is mainly distributed in the range from 0 to 6

Fig. 3 (Color online) Radial density distributions of the 1s (solid line) and 4p states (dashed line)
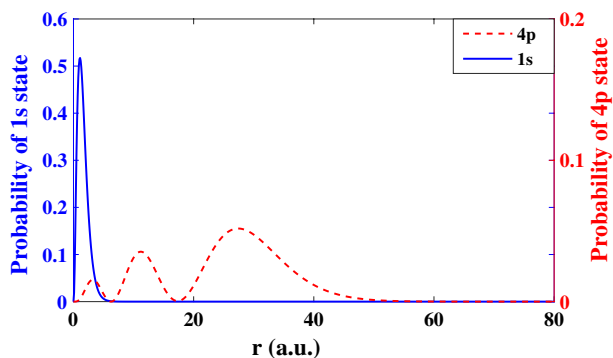
a.u. However, the electrons driven by the CP laser field move circularly around the parent ion, the ionized electrons in this range can barely return to the parent ion. For electrons that can contribute to the harmonic emission but locate far from the nucleus, the corresponding probability density is very small. Therefore, the recombination probability of the electrons in the ground state is low, which leads to the inefficient HHG from the ground-state atom in the CP laser field. By contrast, the excited state (4p state) has much larger probability density for electrons located far from the nucleus (see the dashed line in Fig. 3), even in the range from 45 to 80 a.u. where the electron probability density of the 4p state is already very small. Such a larger electron probability density will also induce the enhancement of HHG from the excited atom. Furthermore, it should be noted that the electron probability density of the 4p state in the range from 6 to 45 a.u. is much larger than that in the range from 45 to 80 a.u. The electrons ionized in the range from 6 to 45 a.u. mainly contribute to the generation of 15th–54th harmonics, while those from 45 to 80 a.u. correspond to 54th–80th harmonics. Due to the larger electron probability density in the range from 6 to 45 a.u., the 15th–54th harmonics therefore show much higher intensity than the 54th–80th harmonics [as shown in Fig. 1b]. It is worth mentioning that in principle, any excited state with larger electron density distribution can be used to generate intense harmonics in the CP laser field. Nevertheless, according to the classical analyses, under the specific laser conditions, only electrons at the specific position can be forced back to the parent ion and contribute to HHG. For excited states with different values of the principal quantum number, the electron probability density at the given position should be different, which therefore could influence the efficiency of the generated harmonics and make a difference in the spectrum structure.

In the following, we demonstrate the generation of near-CP attosecond pulse with HHG from the excited hydrogen atom. As shown in Fig. 2c, g, driven by the CP field, there are only one couple of quantum paths (the short and long one marked by 's' and 'l', respectively) contributing to the harmonic generation. Due to the serious spreading of the electron wavepacket in the continuum (Corkum 1993; Lewenstein et al. 1994), HHG from the long quantum path is much weaker than that from the short one. Then, by superposing several harmonics in the plateau, we can get an IAP. Figure 4 shows the 3D plot of the electric field of the attosecond pulse obtained by superposing the harmonics from 49th to 54th. The x, y components of the attosecond pulse are also plotted. One can see that, one pure attosecond pulse is generated for both the x and y components. The pulse duration of the IAP is about 850 as, which is very close to the Fourier-transform-limited pulse duration (720 as). The slight difference is due to the small positive chirp of the short quantum path, which has broadened the duration of the superposed IAP. Moreover, the electric vector of the
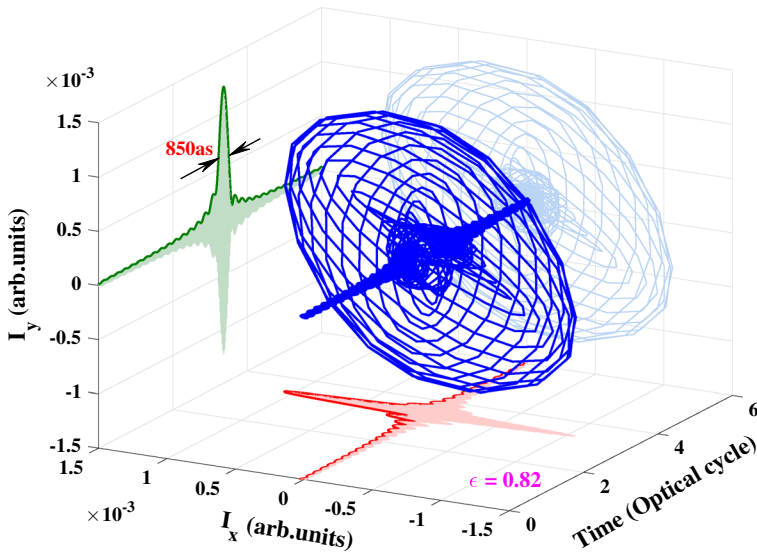
Fig. 4 (Color online) The 3D plot of the electric field of the IAP generated by superposing 49th to 54th harmonics

generated attosecond pulse rotates in the *xy* plane, the ellipticity of this IAP is estimated to be 0.82, which is very close to 1 (a pure CP pulse). Besides, we have also investigated the CEP dependence of the generated IAP in the CP laser field. The results are presented in Fig. 5a–d. Here, the CEP ϕ_0 is chosen to be $-0.1\,\pi$, $-0.2\,\pi$, $-0.3\,\pi$, and $-0.4\,\pi$, and the attosecond pulses are generated by superposing the harmonics from 50th to 55th, 51st to 57th, 53rd to 58th, and 54th to 59th, respectively. It is obvious that IAPs with large ellipticity are generated for all the CEP values. In particular, when the laser CEP is $-0.2\,\pi$, the ellipticity of the generated IAP can reach 0.93, which is a near-CP pulse. It is worth noting that in our simulations, the generation of IAPs in the CP field with large ellipticity is robust with the selection of the excited state. We also investigate the CEP-dependent harmonic spectrum (not shown here), from which we conclude that the harmonic intensities are comparable for different CEPs. The variation of the CEP just makes a slight difference in the detailed structures of the harmonic spectra.

4 Conclusion

In conclusion, we theoretically investigate HHG in a CP laser field with an excited hydrogen atom whose initial state is prepared as a superposition of the ground state $|1s\rangle$ and a excited state $|4p\rangle$. It is shown that the intensity of HHG from the excited atom is 4 to 5 orders of magnitude higher than that from the ground-state atom in the CP laser field and is comparable to that from the ground-state atom in the LP laser field. Our classical and quantum analyses indicate that HHG in the CP laser field mainly originates from the recombination of electrons ionized at non-zero initial positions. The HHG enhancement is due to the higher ionization rate and also the larger probability density of electrons located far from the nucleus of the excited state. The enhanced harmonic spectrum supports the generation of IAP with the ellipticity up to 0.93. Moreover, we
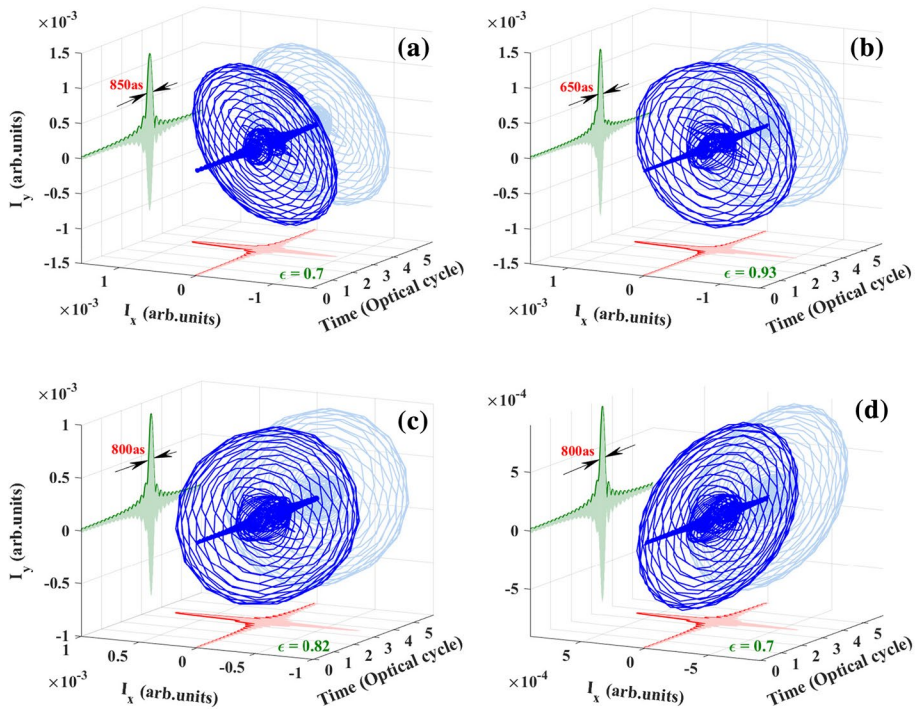
Fig. 5 (Color online) Same to Fig. 4, but for the cases of CEP of **a** − 0.1π, **b** − 0.2π, **c** − 0.3π and **d** − 0.4π, respectively

show that the generation of IAP with large ellipticity is robust against the variation of the CEP of the laser field. This work presents a new access to the generation of near-CP IAP, which will be beneficial for attosecond metrology.

References

Alon, O.E., Averbukh, V., Moiseyev, N.: Selection rules for the high harmonic generation spectra. Phys. Rev. Lett. **80**, 3743 (1998)

Avetissian, H.K., Mkrtchian, G.F.: Multiphoton resonant excitation of atoms in strong laser fields and implementation of coherent superposition states. Phys. Rev. A **66**, 033403 (2002)

Avetissian, H.K., Avchyan, B.R., Mkrtchian, G.F.: Two-color multiphoton resonant excitation of three-level atoms. Phys. Rev. A **74**, 063413 (2006)

Baker, S., Robinson, J.S., Haworth, C.A., Teng, H., Smith, R.A., Chirilă, C.C., Lein, M., Tisch, J.W.G., Marangos, J.P.: Probing proton dynamics in molecules on an attosecond time scale. Science **312**, 424–427 (2006)

Barreau, L., Veyrinas, K., Gruson, V., Weber, S.J., Auguste, T., Hergott, J., Lepetit, F., Carré, B., Houver, J., Dowek, D., Salières, P.: Evidence of depolarization and ellipticity of high harmonics driven by ultra-short bichromatic circularly polarized fields. Nat. Commun. **9**, 4727 (2018)

Barth, I., Manz, J.: Electric ring currents in atomic orbitals and magnetic fields induced by short intense circularly polarized π pulses. Phys. Rev. A **75**, 012510 (2007)

Bleda, E.A., Yavuz, I., Altun, Z., Topcu, T.: High-order-harmonic generation from Rydberg states at fixed Keldysh parameter. Phys. Rev. A **88**, 043417 (2013)

Böwering, N., Lischke, T., Schmidtke, B., Müller, N., Khalil, T., Heinzmann, U.: Asymmetry in photoelectron emission from chiral molecules induced by circularly polarized light. Phys. Rev. Lett. **86**, 1187 (2001)

Burnett, K., Reed, V.C., Cooper, J., Knight, P.L.: Calculation of the background emitted during high-harmonic generation. Phys. Rev. A **45**, 3347 (1992)

Chen, J., Wang, R., Zhai, Z., Chen, J., Fu, P., Wang, B., Liu, W.: Frequency-selected enhancement of high-order-harmonic generation by interference of degenerate Rydberg states in a few-cycle laser pulse. Phys. Rev. A **86**, 033417 (2012)

Chen, J., Wang, K., Long, H., Han, X., Hu, H., Liu, W., Wang, B., Lu, P.: Tungsten disulfide–gold nanohole hybrid metasurfaces for nonlinear metalenses in the visible region. Nano Lett. **18**, 1344–1350 (2018)

Ciappina, M.F., Pérez-Hernández, J.A., Landsman, A.S., Okell, W., Zherebtsov, S., Förg, B., Schötz, J., Seiffert, J.L., Fennel, T., Shaaran, T., Zimmermann, T., Chacón, A., Guichard, R., Zaïr, A., Tisch, J.W.G., Marangos, J.P., Witting, T., Braun, A., Maier, S.A., Roso, L., Krüger, M., Hommelhoff, P., Kling, M.F., Krausz, F., Lewenstein, M.: Attosecond physics at the nanoscale. Rep. Prog. Phys. **80**, 054401 (2017)

Corkum, P.B.: Plasma perspective on strong field multiphoton ionization. Phys. Rev. Lett. **71**, 1994 (1993)

Djotyan, G.P., Bakos, J.S., Sorlei, Zs, Szigeti, J.: Coherent control of atomic quantum states by single frequency-chirped laser pulses. Phys. Rev. A **70**, 063406 (2004)

Dorney, K.M., Ellis, J.L., Hernández-García, C., Hickstein, D.D., Mancuso, C.A., Brooks, N., Fan, T., Fan, G., Zusin, D., Gentry, C., Grychtol, P., Kapteyn, H.C., Murnane, M.M.: Helicity-selective enhancement and polarization control of attosecond high harmonic waveforms driven by bichromatic circularly polarized laser fields. Phys. Rev. Lett. **119**, 063201 (2017)

Ellis, J.L., Dorney, K.M., Hickstein, D.D., Brooks, N.J., Gentry, C., Hernández-García, C., Zusin, D., Shaw, J.M., Nguyen, Q.L., Mancuso, C.A., Jansen, G.S.M., Witte, S., Kapteyn, H.C., Murnane, M.M.: High harmonics with spatially varying ellipticity. Optica **5**, 479–485 (2018)

Fan, T., Grychtol, P., Knut, R., Hernández-García, C., Hickstein, D.D., Zusin, D., Gentry, C., Dollar, F.J., Mancuso, C.A., Hogle, C.W., Kfir, O., Legut, D., Carva, K., Ellis, J.L., Dorney, K.M., Chen, C., Shpyrko, O.G., Fullerton, E.E., Cohen, O., Oppeneer, P.M., Milošević, D.B., Becker, A., Jaroń-Becker, A.A., Popmintchev, T., Murnane, M.M., Kapteyn, H.C.: Bright circularly polarized soft X-ray high harmonics for X-ray magnetic circular dichroism. Proc. Natl. Acad. Sci. USA **112**, 14206–14211 (2015)

Feit, M.D., Fleck, J.A., Steiger, A.: Solution of the Schrödinger equation by a spectral method. J. Comput. Phys. **47**, 412–433 (1982)

Feng, L.: Molecular harmonic extension and enhancement from H_2^+ ions in the presence of spatially inhomogeneous fields. Phys. Rev. A **92**, 053832 (2015)

Feng, L., Chu, T.: Generation of an isolated sub-40-as pulse using two-color laser pulses: Combined chirp effects. Phys. Rev. A **84**, 053853 (2011)

Feng, L., Li, Y., Feng, Y.A.: Nano-plasmonic-pump-probe effect on the intensity enhancement of attosecond pulse from hydrogen molecular ion. Laser Phys. Lett. **15**, 115301 (2018)

Ferré, A., Handschin, C., Dumergue, M., Burgy, F., Comby, A., Descamps, D., Fabre, B., Garcia, G.A., Géneaux, R., Merceron, L., Mével, E., Nahon, L., Petit, S., Pons, B., Staedter, D., Weber, S., Ruchon, T., Blanchet, V., Mairesse, Y.: A table-top ultrashort light source in the extreme ultraviolet for circular dichroism experiments. Nat. Photonics **9**, 93–98 (2014)

Gaumnitz, T., Jain, A., Pertot, Y., Huppert, M., Jordan, I., Ardana-Lamas, F., Wörner, H.J.: Streaking of 43-attosecond soft-X-ray pulses generated by a passively CEP-stable mid-infrared driver. Opt. Express **25**, 27506–27518 (2017)

Ghimire, S., DiChiara, A.D., Sistrunk, E., Agostini, P., DiMauro, L.F., Reis, D.A.: Observation of high-order harmonic generation in a bulk crystal. Nat. Phys. **7**, 138–141 (2011)

Goulielmakis, E., Loh, Z.H., Wirth, A., Santra, R., Rohringer, N., Yakovlev, V.S., Zherebtsov, S., Pfeifer, T., Azzeer, A.M., Kling, M.F., Leone, S.R., Krausz, F.: Real-time observation of valence electron motion. Nature **466**, 739–743 (2010)

Gui, D., Ji, L., Muhammad, A., Li, W., Cai, W., Li, Y., Li, X., Wu, X., Lu, P.: Jahn-Teller effect on framework flexibility of hybrid organic-inorganic perovskites. J. Phys. Chem. Lett. **9**, 751–755 (2018)

He, M., Li, Y., Zhou, Y., Li, M., Cao, W., Lu, P.: Direct visualization of valence electron motion using strong-field photoelectron holography. Phys. Rev. Lett. **120**(13), 133204 (2018a)

He, L., Zhang, Q., Lan, P., Cao, W., Zhu, X., Zhai, C., Wang, F., Shi, W., Li, M., Bian, X., Lu, P., Bandrauk, A.D.: Monitoring ultrafast vibrational dynamics of isotopic molecules with frequency modulation of high-order harmonics. Nat. Commun. **9**, 1108 (2018b)

He, L., Lan, P., Le, A.-T., Wang, B., Zhu, X., Lu, P., Lin, C.D.: Real-time observation of molecular spinning with angular high-harmonic spectroscopy. Phys. Rev. Lett. **121**, 163201 (2018c)

He, Y., He, L., Lan, P., Wang, B., Li, L., Zhu, X., Cao, W., Lu, P.: Molecular rotation movie filmed with high-harmonic generation. arXiv:1902.05662 [physics.optics] (2019)

Hernández-García, C., Durfee, C.G., Hickstein, D.D., Popmintchev, T., Meier, A., Murnane, M.M., Kapteyn, H.C., Sola, I.J., Jaron-Becker, A., Becker, A.: Schemes for generation of isolated attosecond pulses of pure circular polarization. Phys. Rev. A **93**, 043855 (2016)

Hickstein, D.D., Dollar, F.J., Grychtol, P., Ellis, J.L., Knut, R., Hernández-García, C., Zusin, D., Gentry, C., Shaw, J.M., Fan, T., Dorney, K.M., Becker, A., Jaroń-Becker, A., Kapteyn, H.C., Murnane, M.M., Durfee, C.G.: Non-collinear generation of angularly isolated circularly polarized high harmonics. Nat. Photonics **9**, 743–750 (2015)

Hu, S.X., Collins, L.A.: High-order harmonic generation from intense laser-driven inner electrons of Rydberg atoms. Phys. Rev. A **69**, 033405 (2004)

Huang, P.C., Hernández-García, C., Huang, J., Huang, P., Lu, C., Rego, L., Hickstein, D.D., Ellis, J.L., Jaron-Becker, A., Becker, A., Yang, S., Durfee, C.G., Plaja, L., Kapteyn, H.C., Murnane, M.M., Kung, A.H., Chen, M.: Polarization control of isolated high-harmonic pulses. Nat. Photonics **12**, 349–354 (2018)

Itatani, J., Levesque, J., Zeidler, D., Niikura, H., Pépin, H., Kieffer, J.C., Corkum, P.B., Villeneuve, D.M.: Tomographic imaging of molecular orbitals. Nature **432**, 867–871 (2004)

Jiménez-Galán, Á., Zhavoronkov, N., Schloz, M., Morales, F., Ivanov, M.: Time-resolved high harmonic spectroscopy of dynamical symmetry breaking in bi-circular laser fields: the role of Rydberg states. Opt. Express **25**, 22880–22896 (2017)

Kfir, O., Grychtol, P., Turgut, E., Knut, R., Zusin, D., Popmintchev, D., Popmintchev, T., Nembach, H., Shaw, J.M., Fleischer, A., Kapteyn, H., Murnane, M., Cohen, O.: Generation of bright phase-matched circularly-polarized extreme ultraviolet high harmonics. Nat. Photonics **9**, 99–105 (2015)

Kienberger, R., Goulielmakis, E., Uiberacker, M., Baltuska, A., Yakovlev, V., Bammer, F., Scrinzi, A., Westerwalbesloh, Th, Kleineberg, U., Heinzmann, U., Drescher, M., Krausz, F.: Atomic transient recorder. Nature **427**, 817–821 (2004)

Kim, S., Jin, J., Kim, Y.J., Park, I.Y., Kim, Y., Kim, S.W.: High-harmonic generation by resonant plasmon field enhancement. Nature **453**, 757–760 (2008)

Krausz, F., Ivanov, M.: Attosecond physics. Rev. Mod. Phys. **81**, 163–234 (2009)

Krüger, M., Lemell, C., Wachter, G., Burgdörfer, J., Hommelhoff, P.: Attosecond physics phenomena at nanometric tips. J. Phys. B **51**, 172001 (2018)

Lan, P., Ruhmann, M., He, L., Zhai, C., Wang, F., Zhu, X., Zhang, Q., Zhou, Y., Li, M., Lein, M., Lu, P.: Attosecond probing of nuclear dynamics with trajectory-resolved high-harmonic spectroscopy. Phys. Rev. Lett. **119**, 033201 (2017)

Lewenstein, M., Balcou, P., Ivanov, M.Y., L'Huillier, A., Corkum, P.B.: Theory of high-harmonic generation by low-frequency laser fields. Phys. Rev. A **49**, 2117 (1994)

Li, J., Ren, X., Yin, Y., Zhao, K., Chew, A., Cheng, Y., Cunningham, E., Wang, Y., Hu, S., Wu, Y., Chini, M., Chang, Z.: 53-attosecond X-ray pulses reach the carbon K-edge. Nat. Commun. **8**, 186 (2017a)

Li, L., Wang, Z., Li, F., Long, H.: Efficient generation of highly elliptically polarized attosecond pulses. Opt. Quant. Electron. **49**(2), 73 (2017b)

Li, L., Lan, P., He, L., Zhu, X., Chen, J., Lu, P.: Scaling law of high harmonic generation in the framework of photon channels. Phys. Rev. Lett. **120**(22), 223203 (2018)

Li, L., Lan, P., Zhu, X., Huang, T., Zhang, Q., Lein, M., Lu, P.: Reciprocal-space-trajectory perspective on high harmonic generation in solids. Phys. Rev. Lett. **122**(19), 193901 (2019a)

Li, M., Xie, H., Cao, W., Luo, S., Tan, J., Feng, Y., Du, B., Zhang, W., Li, Y., Zhang, Q., Lan, P., Zhou, Y., Lu, P.: Photoelectron holographic interferometry to probe the longitudinal momentum offset at the tunnel exit. Phys. Rev. Lett. **122**(18), 183202 (2019b)

Li, J., Zhang, Q., Li, L., Zhu, X., Huang, T., Lan, P., Lu, P.: Orientation dependence of high-order harmonic generation in nanowire. Phys. Rev. A **99**(3), 033421 (2019c)

Liu, W., Li, X., Song, Y., Zhang, C., Han, X., Long, H., Wang, B., Wang, K., Lu, P.: Cooperative enhancement of two-photon-absorption-induced photoluminescence from a 2D perovskite-microsphere hybrid dielectric structure. Adv. Funct. Mater. **28**, 1707550 (2018)

Liu, K., Luo, S., Li, M., Li, Y., Feng, Y., Du, B., Zhou, Y., Lu, P., Barth, I.: Detecting and characterizing the nonadiabaticity of laser-induced quantum tunneling. Phys. Rev. Lett. **122**(5), 053202 (2019a)

Liu, Y., Tan, J., He, M., Xie, H., Qin, Y., Zhao, Y., Li, M., Zhou, Y., Lu, P.: Photoelectron holographic interferences from multiple returning in strong-field tunneling ionization. Opt. Quant. Electron. **51**(5), 145 (2019b)

López-Flores, V., Arabski, J., Stamm, C., Halté, V., Pontius, N., Beaurepaire, E., Boeglin, C.: Time-resolved x-ray magnetic circular dichroism study of ultrafast demagnetization in a CoPd ferromagnetic film excited by circularly polarized laser pulse. Phys. Rev. B **86**, 014424 (2012)

Luo, S., Li, M., Xie, W., Liu, K., Feng, Y., Du, B., Zhou, Y., Lu, P.: Exit momentum and instantaneous ionization rate of nonadiabatic tunneling ionization in elliptically polarized laser fields. arXiv:1905.06162 [physics.atom-ph] (2019)

Ma, X., Zhou, Y., Chen, Y., Li, M., Li, Y., Zhang, Q., Lu, P.: Timing the release of the correlated electrons in strong-field nonsequential double ionization by circularly polarized two-color laser fields. Opt. Express **27**(3), 1825–1837 (2019)

Mauger, F., Bandrauk, A.D., Kamor, A., Uzer, T., Chandre, C.: Quantum-classical correspondence in circularly polarized high harmonic generation. J. Phys. B **47**(4), 041001 (2014)

Medišauskas, L., Wragg, J., van der Hart, H., Ivanov, M.Y.: Generating isolated elliptically polarized attosecond pulses using bichromatic counterrotating circularly polarized laser fields. Phys. Rev. Lett. **115**, 153001 (2015)

Milošević, D.B.: Generation of elliptically polarized attosecond pulse trains. Opt. Lett. **40**, 2381–2384 (2015)

Pfeifer, T., Gallmann, L., Abel, M.J., Nagel, P.M., Neumark, D.M., Leone, S.R.: Heterodyne mixing of laser fields for temporal gating of high-order harmonic generation. Phys. Rev. Lett. **97**, 163901 (2006)

Popmintchev, T., Chen, M.C., Popmintchev, D., Arpin, P., Brown, S., Ališauskas, S., Andriukaitis, G., Balčiunas, T., Mücke, O.D., Pugzlys, A., Baltuška, A., Shim, B., Schrauth, S.E., Gaeta, A., Hernández-GarcÍa, C., Plaja, L., Becker, A., Jaron-Becker, A., Murnane, M.M., Kapteyn, H.C.: Bright coherent ultrahigh harmonics in the keV x-ray regime from mid-infrared femtosecond lasers. Science **336**, 1287–1291 (2012)

Qin, Y.N., Li, M., Li, Y., He, M., Luo, S., Liu, Y., Zhou, Y., Lu, P.: Asymmetry of the photoelectron momentum distribution from molecular ionization in elliptically polarized laser pulses. Phys. Rev. A **99**(1), 013431 (2019)

Sansone, G., Benedetti, E., Calegari, F., Vozzi, C., Avaldi, L., Flammini, R., Poletto, L., Villoresi, P., Altucci, C., Velotta, R., Stagira, S., Silvestri, S.D., Nisoli, M.: Isolated single-cycle attosecond pulses. Science **314**, 443–446 (2006)

Schultze, M., Ramasesha, K., Pemmaraju, C., Sato, S., Whitmore, D., Gandman, A., Prell, J.S., Borja, L., Prendergast, D., Yabana, K., Neumark, D.M., Leone, S.R.: Attosecond band-gap dynamics in silicon. Science **346**, 1348–1352 (2014)

Tan, J., Zhou, Y., He, M., Chen, Y., Ke, Q., Liang, J., Zhu, X., Li, M., Lu, P.: Determination of the ionization time using attosecond photoelectron interferometry. Phys. Rev. Lett. **121**(25), 253203 (2018)

Tan, J., Zhou, Y., He, M., Ke, Q., Liang, J., Li, Y., Li, M., Lu, P.: Time-resolving tunneling ionization via strong-field photoelectron holography. Phys. Rev. A **99**(3), 033402 (2019)

Teichmann, S.M., Silva, F., Cousin, S.L., Hemmer, M., Biegert, J.: 0.5-keV soft x-ray attosecond continua. Nat. Commun. **7**, 11493 (2016)

Vampa, G., Hammond, T.J., Thiré, N., Schmidt, B.E., Légaré, F., McDonald, C.R., Brabec, T., Corkum, P.B.: Linking high harmonics from gases and solids. Nature (London) **522**, 462–464 (2015)

Wang, Z., He, L., Luo, J., Lan, P., Lu, P.: High-order harmonic generation from Rydberg atoms in inhomogeneous fields. Opt. Express **22**, 25909–25922 (2014)

Wang, B., He, L., Yuan, H., Zhang, Q., Lan, P., Lu, P.: Carrier-envelope phase-dependent molecular high-order harmonic generation from H_2^+ in a multi-cycle regime. Opt. Express **26**(25), 33440–33452 (2018)

Wang, R., Zhang, Q., Li, D., Xu, S., Cao, P., Zhou, Y., Cao, W., Lu, P.: Identification of tunneling and multiphoton ionization in intermediate Keldysh parameter regime. Opt. Express **27**(5), 6471–6482 (2019)

Xie, X., Scrinzi, A., Wickenhauser, M., Baltuška, A., Barth, I., Kitzler, M.: Internal momentum state mapping using high harmonic radiation. Phys. Rev. Lett. **101**, 033901 (2008)

Yuan, K.J., Bandrauk, A.D.: Single circularly polarized attosecond pulse generation by intense few cycle elliptically polarized laser pulses and terahertz fields from molecular media. Phys. Rev. Lett. **110**, 023003 (2013)

Yuan, H., He, L., Wang, F., Wang, B., Zhu, X., Lan, P., Lu, P.: Tomography of asymmetric molecular orbitals with a one-color inhomogeneous field. Opt. Lett. **43**, 931–934 (2018)

Zhai, Z., Chen, J., Yan, Z.C., Fu, P., Wang, B.: Direct probing of electronic density distribution of a Rydberg state by high-order harmonic generation in a few-cycle laser pulse. Phys. Rev. A **82**, 043422 (2010)

Zhai, Z., Zhu, Q., Chen, J., Yan, Z.C., Fu, P., Wang, B.: High-order harmonic generation with Rydberg atoms by using an intense few-cycle pulse. Phys. Rev. A **83**, 043409 (2011)

Zhang, X., Zhu, X., Wang, D., Li, L., Liu, X., Liao, Q., Lan, P., Lu, P.: Ultrafast oscillating-magnetic-field generation based on electronic-current dynamics. Phys. Rev. A **99**(1), 013414 (2019)

Zhou, Y., Huang, C., Liao, Q., Lu, P.: Classical simulations including electron correlations for sequential double ionization. Phys. Rev. Lett. **109**(5), 053004 (2012)

Publisher's Note Springer Nature remains neutral with regard to jurisdictional claims in published maps and institutional affiliations.